03,09

# Characterization of wide-bandgap layers in laser structures based on CdHgTe

© M.S. Ruzhevich[1], K.D. Mynbaev[2], N.L. Bazhenov[2], M.V. Dorogov[1], S.A. Dvoretskii[3], N.N. Mikhailov[3], V.G. Remesnik[3], I.N. Uzhakov[3]

[1] ITMO University,
St. Petersburg, Russia
[2] Ioffe Institute,
St. Petersburg, Russia
[3] Rzhanov Institute of Semiconductor Physics, Siberian Branch, Russian Academy of Sciences,
Novosibirsk, Russia

E-mail: mynkad@mail.ioffe.ru

*Received December 12, 2022*
*Revised December 12, 2022*
*Accepted December 22, 2022*

The results of a study of the optical and structural properties of wide-bandgap ($x \sim 0.7$) layers in laser heterostructures based on $Cd_xHg_{1-x}Te$ solid solutions grown by molecular beam epitaxy on (013)GaAs substrates, as well as epitaxial films similar to these layers in chemical composition, are presented. It is shown that the position of the maximum of the photoluminescence spectrum and the nature of its temperature shift are related to the disordering of the composition of the solid solution. Shallow and deep acceptor levels were found in the bandgap. The possible influence of disordering and acceptor levels in laser structures on the energy spectrum of carriers is discussed.

**Keywords:** CdHgTe, laser structures, photoluminescence, defects, structural properties.

DOI: 10.21883/PSS.2023.03.55580.552

## 1. Introduction

Quantum well (QW) heterostructures based on $Cd_xHg_{1-x}Te$ (MCT) have been actively studied in recent years with the aim of creating infrared (IR) semiconductor lasers on their basis. MCT-based lasers that use interband transitions to generate radiation are expected to compete with quantum-cascade lasers both in the long-wavelength (wavelength $\lambda > 15\,\mu$m) [1], and in the medium wave ($\lambda = 3-6\,\mu$m) [2] IR bands. Laser structures (LS) based on MCT with optical pumping, multiple QWs and waveguides are currently being investigated [1–3]. When creating them, the technological problem of both obtaining a QW material based on pure HgTe and forming structurally perfect wide-gap (barrier and waveguide) layers with a given composition (CdTe mole fraction) $x$ and doping level is solved. These layers provide electronic confinement, form a waveguide, and determine, along with the parameters of the QW themselves, the dispersion law of carriers in the well, which is a key factor in suppressing Auger recombination for efficient generation of laser radiation in an MCT-based LS [4,5].

Barrier and waveguide layers in MCT-based LS are usually made of material with $x \approx 0.6-0.7$ [4,5]. It should be taken into account, however, that the MCT technology has been dveloped for many years for „small" $x$ ($0.2-0.3$), which are in demand in the manufacture of photodetectors, and the growth of relatively thick (for LS of long-wavelength IR-range — more than $10\,\mu$m) layers of wide-gap compositions requires the use of special technological methods [6], and, in general, optimization. We have previously compared the properties of wide-gap MCT samples grown by molecular beam epitaxy (MBE), liquid-phase epitaxy, and vertically directed crystallization [7,8]. This work reports the results of a study of the optical and structural properties of the MBE-grown material intended for the creation of wide-gap layers in a LS.

## 2. Experimental procedure

The objects of study were LS with multiple QW and barrier and waveguide layers with $x \approx 0.7$; for comparison, test epitaxial films (EF) of similar compositions grown by the same method were studied. All samples were grown on (013) GaAs substrates with ZnTe and CdTe [6] buffer layers. The parameters of the samples are given in the table, where the value of $x$ and the thickness of the layers are indicated according to the *in situ* ellipsometry data. These parameters were also controlled using energy-dispersive X-ray spectroscopy (EDS) on a TESCAN MIRA 3 electron microscope with an ULTIM MAX 100 detector manufactured by Oxford Instruments.

The LS growth ended with the formation of a protective surface layer of CdTe with a thickness of $25-50$ nm. On 1222, 1223, 1224, and 1227 EF samples, a thin (up to 200 nm) HgTe layer was grown on the surface, which was used to form electrical contacts when measuring the

Parameters of samples grown on (013) GaAs substrates with ZnTe and CdTe buffer layers

| sample | Type of structure (number×QW width, nm) | $x$ in the investigated layer(s) | Thickness of wide-gap LS/EF layers, $\mu$m |
|---|---|---|---|
| 0225 | LS (11×7.1) | 0.70 | 7.3 |
| 0220 | LS (10×7.1) | 0.70 | 7.0 |
| 0423 | LS (10×2.7) | 0.74 | 0.7 |
| 0429 | LS (3×2.7) | 0.73 | 0.7 |
| 0417 | EF | 0.74 | 5.0 |
| 1222 | EF | 0.73 | 3.0 |
| 1223 | EF | 0.71 | 3.0 |
| 1224 | EF | 0.71 | 3.0 |
| 1227 | EF | 0.72 | 3.0 |

Hall coefficient and conductivity. EF 0417 and 1222 were undoped. EF 1223, 1224 and 1227 were doped with indium during growth to an electron concentration in the range of $2.0 \cdot 10^{16}\,\mathrm{cm}^{-3}$ (EF 1223) to $1.5 \cdot 10^{18}\,\mathrm{cm}^{-3}$ (EF 1227). EF 0417 was grown using growth rate calibration as described in [6]. Optical transmission (OT) and photoluminescence (PL) methods were used in optical studies. OT spectra were recorded at $T = 300\,\mathrm{K}$ using a Fourier spectrometer InfraLUM-801. The PL spectra were recorded in the temperature range $T = 4.2-300\,\mathrm{K}$ using an MDR-23 monochromator upon excitation by a semiconductor laser ($\lambda = 1.03\,\mu\mathrm{m}$) and recording the signal with a germanium photodiode using a lock-in amplifier. In the LS under study, the thickness of the barrier layers between the QW was $\sim 25\,\mathrm{nm}$; therefore, the exciting PL radiation was absorbed mainly by the waveguide layers. The table shows the averaged (with allowance for a small ($\sim 5\%$) change in the composition during growth recorded by ellipsometry data) parameters of these layers. In LS 0423 and 0429 the material of the same chemical composition was used in the barrier layers as in the waveguide layers. In structures 0225 and 0220, the barriers were made of material with $x \approx 0.62$ and $x \approx 0.57$, respectively.

## 3. Results and discussion

Fig. 1 shows the OT spectra of the number of the samples. These spectra are typical of samples grown by MBE [7–9] and are characterized by sharp transmission edges and pronounced interference fringes at low wavenumbers. Before recording the EF 1222, 1223, 1224, and 1227 spectra, the HgTe layer was removed from the surface by chemical etching; the spectra of these samples have „a classical“ shape in comparison with the transmission spectra of the LS, where several layers of different chemical composition were present, and the edge had a complex shape (Fig. 1, *a*). The position of the main edge of the OT for all structures generally corresponded to the values of the chemical composition determined from ellipsometry data. For the EF 1227 sample doped with indium to a concentration of $1.5 \cdot 10^{18}\,\mathrm{cm}^{-3}$, absorption by free carriers is noticeable in the OT spectrum at low wavenumbers (Fig. 1, *b*).

Figure 2, *a* shows the normalized PL spectra of some of the investigated LS recorded at $T = 4.2\,\mathrm{K}$. The spectrum of LS 0429 (not shown) contained one band, while the spectra *1* and *2* of structures 0225 and 0220, respectively, were best approximated by two bands separated by $\sim 12\,\mathrm{meV}$ (examples of approximations are given in [7,8]). The full width at half maximum (FWHM) of the high-energy bands („edge“ PL) were $\sim 16\,\mathrm{meV}$, and the low-energy bands, $\sim 30\,\mathrm{meV}$. The spectrum of LS 0423 also contained two bands. The FWHM of the high-energy band here was $\sim 18\,\mathrm{meV}$, the low-energy band was much wider. As the temperature increased, this band became more pronounced. Its intensity increased to $T \sim 130\,\mathrm{K}$; then this band disappeared. A similar effect was previously observed by us for EFs with $x = 0.3-0.4$ grown on Si substrates [10]. Just as in the latter case, the depth of the level responsible for the appearance of the low-energy band in LS 0423 was $\sim 70\,\mathrm{meV}$. The PL spectra of the EF samples at $T = 4.2\,\mathrm{K}$ (not shown), similarly to the spectra of LS 0225 and 0220, also indicated the presence of shallow acceptor states with a depth of $\sim 15-20\,\mathrm{meV}$. The FWHM of the high-energy lines in these spectra ranged from 17 to 27 meV and increased with increasing indium concentration. At $T = 300\,\mathrm{K}$, the PL spectra were single bands with FWHM from 60 to 70 meV. The contribution of barrier layers to the PL signal for LS 0225 and 0220, as expected, was not observed.

Figure 2, *b* shows the temperature dependences of the positions of the „edge“ PL peaks $E_{\mathrm{PL}}(T)$ for some samples. For samples LS 1223 and 1224 these dependences were similar and the figure shows the dependence only for LS 1224. For EF 0417, as was shown earlier [8], high-energy (FWHM 17 meV) and low-energy (FWHM 25 meV) bands could be assigned „to edge“ PL of two layers of different compositions (surface layer $x = 0.74$-thick $5\,\mu\mathrm{m}$ and layer $x = 0.70$ near the substrate $1\,\mu\mathrm{m}$-thick). The high-energy PL band of the sample 0417 was observed only up to a temperature of $\sim 70\,\mathrm{K}$, the only PL band of the EF 1222 — up to 90 K.

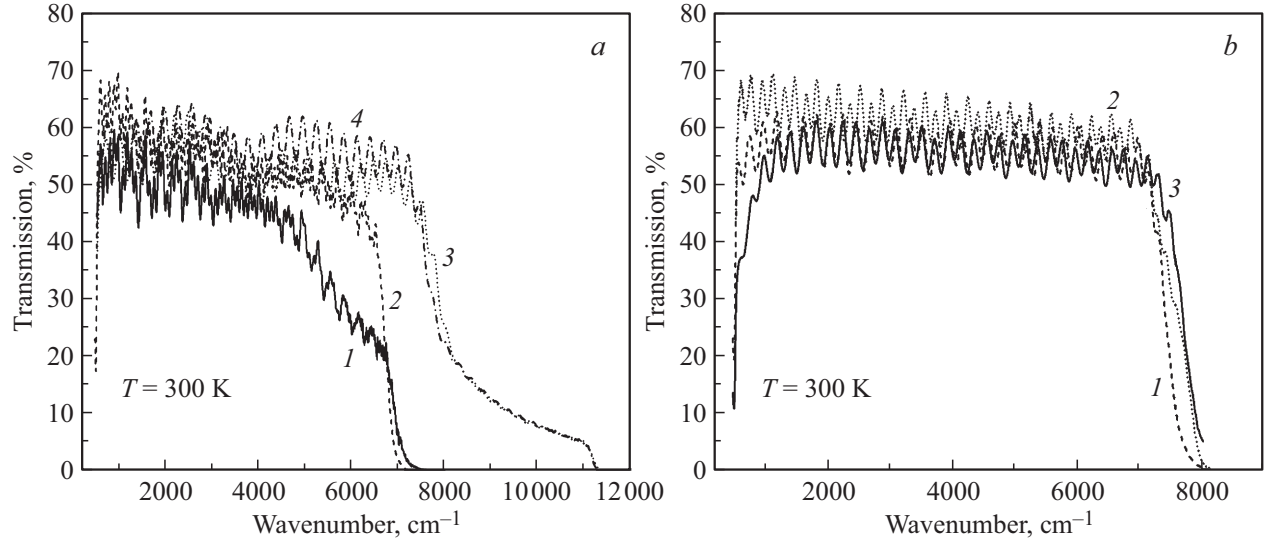


**Figure 1.** Optical transmission spectra of laser structures 0220 (*1*), 0225 (*2*), 0423 (*3*) and 0429 (*4*) (*a*), as well as samples of epitaxial films 1223 (*1*), 0417 (*2*) and 1227 (*3*) (*b*).

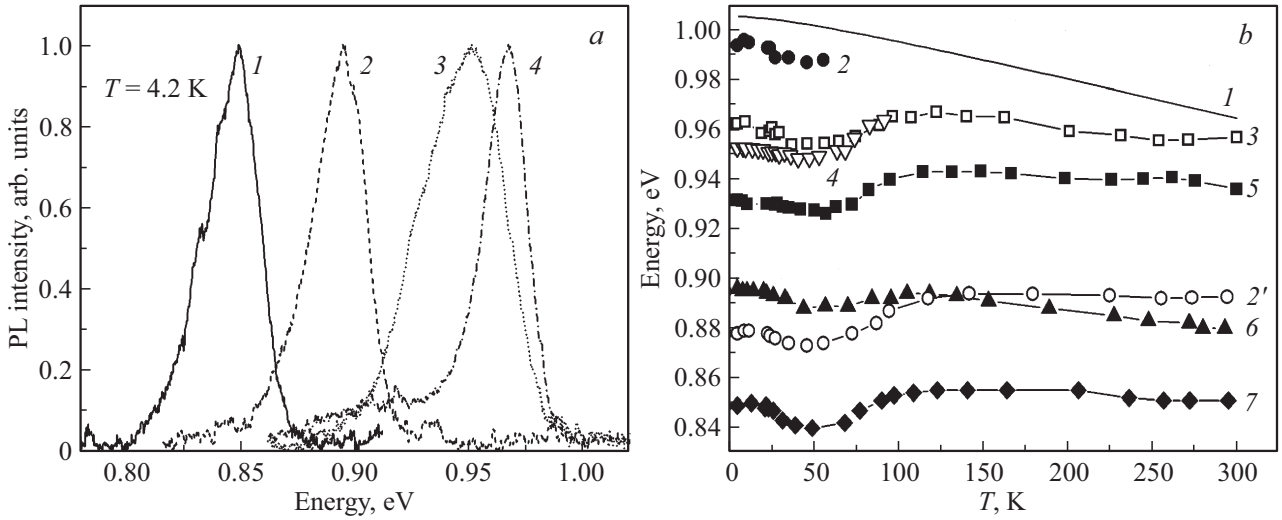


**Figure 2.** Normalized PL spectra of LS 0225 (spectrum *1*), 0220 (*2*), 0429 (*3*) and 0423 (*4*) (*a*), and the calculated dependence of the band gap $E_g(T)$ for MCT with $x = 0.7$ (line *1*) and the experimental dependences of the peak position of high-energy PL bands $E_{PL}(T)$ for EF 0417 (*2* and *2′*), 1227 (*3*), 1222 (*4*), 1223 (*5*), and LS 0220 (*6*) and 0225 (*7* ) (*b*).

When analyzing the obtained results, two circumstances attract attention. The first of them is related to the discrepancy between the energies of the PL peaks in the entire studied temperature range and the chemical composition of the material under study according to ellipsometry and OT data. Due to the poor locality of the used EDS technique (the signal was collected from a region with a diameter of $\sim 1\,\mu$m), the control of the composition by this method was carried out only for EF along the cleavage of the samples. Precise quantitative determination of the composition of the solid solution was hindered by the presence of gallium and arsenic lines from the substrate in the spectra, however, the EDS data qualitatively confirmed an increase in $x$ in the EF series from 1223 (1224) to 1227 and then to 1222 (see table). At the same time, for example, at the same value $x$ of the peaks of the PL spectra of EF 1222 had an energy lower than that for EF 1227 (Fig. 2, *b*), and the values of $E_{PL}$ were significantly less than the values of $E_g$ (calculated from the data [11]) even for the composition $x \approx 0.70$ (line *1* in Fig. 2, *b*). This indicated that the high-energy PL lines in the samples under study were due to optical transitions caused by the recombination of excitons localized on composition fluctuations [12] and, accordingly, showed a significant disordering of the solid solution. The last statement, as shown by X-ray diffraction and microscopic studies of such material [7,8,13,14], cannot

always be directly related to its structural quality. The potential influence of this disordering on the energy spectrum of carriers in LS should be the subject of additional studies.

The second circumstance is associated with the presence of shallow and deep acceptor levels in the studied material, which was detected from the PL data. Deep levels with an energy of $\sim 70$ meV were detected in EF 0417 and LS 0423, shallow (from 10 to 20 meV), — in LS 0220 and 0225, as well as in EF 1222, 1223, 1224 and 1227. As noted previously [7,13], the presence of such lines in the PL spectra is not characteristic of MCT structures with $x \approx 0.3-0.4$ grown using this technology on GaAs substrates. Thus, the appearance of these states may be related to the growth conditions, which are different for a material with small and large $x$. In view of the fact that the energy used for optical pumping of an MCT-based LS is substantially less than the value of $E_g$ in barrier and waveguide layers [1–4] the presence of even deep levels in wide-gap layers should not lead to the manifestation of the contribution of undesirable recombination centers. However, taking into account the sensitivity of the threshold of Auger processes in LS based on MCT to the energy spectrum of carriers, as well as the prospects for creating injection lasers based on MCT, this issue also requires further study.

## 4. Conclusion

The results of characterization of wide-gap layers in laser structures based on CdHgTe solid solutions grown by molecular beam epitaxy showed that, while the material nominally corresponds to the declared chemical composition, it is characterized by disordering of the solid solution, which affects the position of the maximum of the luminescence spectrum and its temperature shift. Photoluminescent studies made it possible to detect both shallow and deep states in the band gap, which are not typical of CdHgTe films with smaller composition grown by this method on GaAs substrates. The influence of disordering and the presence of acceptor states on the energy spectrum of carriers in laser structures requires further study.

### Conflict of interest

The authors declare that they have no conflict of interest.

## References

[1] V.V. Rumyantsev, A.A. Dubinov, V.V. Utochkin, M.A. Fadeev, V.Ya. Aleshkin, A.A. Razova, N.N. Mikhailov, S.A. Dvoretsky, V.I. Gavrilenko, S.V. Morozov. Appl. Phys. Lett. **121**, *18*, 182103 (2022).

[2] V.V. Utochkin, K.E. Kudryavtsev, A.A. Dubinov, M.A. Fadeev, V.V. Rumyantsev, A.A. Razova, E.V. Andronov, V.Ya. Aleshkin, V.I. Gavrilenko, N.N. Mikhailov, S.A. Dvoretsky, F. Teppe, S.V. Morozov. Nanomaterials **12**, *15*, 2599 (2022).

[3] L.A. Kushkov, V.V. Utochkin, V.Ya. Aleshkin, A.A. Dubinov, K.E. Kudryavtsev, V.I. Gavrilenko, N.S. Kulikov, M.A. Fadeev, V.V. Rumyantsev, N.N. Mikhailov, S.A. Dvoretsky, A.A. Razova, S.V. Morozov. Semiconductors **54**, 1365 (2020).

[4] M.A. Fadeev, A.A. Dubinov, V.Ya. Aleshkin, V.V. Rumyantsev, V.V. Utochkin, V.I. Gavrilenko, F. Teppe, H.- V. Hübers, N.N. Mikhailov, S.A. Dvoretsky, S.V. Morozov, Quantum Electron. **49**, *6*, 556 (2019).

[5] V.Ya. Aleshkin, V.V. Rumyantsev, K.E. Kudryavtsev, A.A. Dubinov, V.V. Utochkin, M.A. Fadeev, G. Alymov, N.N. Mikhailov, S.A. Dvoretsky, F. Teppe, V.I. Gavrilenko, S.V. Morozov. J. Appl. Phys. **129**, *13*, 133106 (2021).

[6] V.A. Shvets, N.N. Mikhailov, D.G. Ikusov, I.N. Uzhakov, S.A. Dvoretsky. Optics and Spectroscopy **127**, 340 (2019).

[7] K.D. Mynbaev, N.L. Bazhenov, A.M. Smirnov, N.N. Mikhailov, V.G. Remesnik, M.V. Yakushev. Semiconductors **54**, 1561 (2020).

[8] K.D. Mynbaev, A.M. Smirnov, N.L. Bazhenov, N.N. Mikhailov, V.G. Remesnik, M.V. Yakushev. J. Electron. Mater. **49**, *8*, 4642 (2020).

[9] F.-Y. Yue, S.-Y. Ma, J. Hong, P.-X. Yang, C.-B. Jing, Y. Chen, J.-H. Chu. Chin. Phys. B **28**, *1*, 017104 (2019).

[10] K.D. Mynbaev, S.V. Zablotsky, A.V. Shilyaev, N.L. Bazhenov, M.V. Yakushev, D.V. Marin, V.S. Varavin, S.A. Dvoretsky. Semiconductors **54**, 208 (2016).

[11] C.R. Becker, V. Latussek, A. Pfeuer-Jeschke, G. Landwehr, L.W. Molenkamp. Phys. Rev. B **62**, *15*, 10353 (2000).

[12] K.D. Mynbaev, N.L. Bazhenov, V.I. Ivanov-Omskii, N.N. Mikhailov, M.V. Yakushev, A.V. Sorochkin, V.G. Remesnik, S.A. Dvorestkiy, V.S. Varavin, Yu.G. Sidorov. Semiconductors **45**, 872 (2011).

[13] D.A. Andryushchenko, M.S. Ruzevich, A.M. Smirnov, N.L. Bazhenov, K.D. Mynbaev, V.G. Remesnik. Semiconductors **56**, *13*, 2063 (2022).

[14] N. Mikhailov, V. Shvets, D. Ikusov, I. Uzhakov, S. Dvoretsky, K. Mynbaev, P. Dluzewski, J. Morgiel, Z. Swiatek, O. Bonchyk, I. Izhnin. Phys. Status Solidi B **257**, *5*, 1900598 (2020).

*Translated by E.Potapova*